

## Collective properties of hadrons in comparison of models prediction in $pp$ collisions at 7 TeV

Muhammad Ajaz<sup>a,\*</sup>, Ahmed M. Khubrani<sup>b</sup>, Muhammad Waqas<sup>c,\*</sup>, Abd Al Karim Haj Ismail<sup>d,e</sup>, Elmuez A. Dawi<sup>d,e</sup>

<sup>a</sup> Department of Physics, Abdul Wali Khan University Mardan, Mardan 23200, Pakistan

<sup>b</sup> Department of Physics, Faculty of Science, Jazan University, Jazan 45142, Saudi Arabia

<sup>c</sup> School of Nuclear Science and Technology, University of Chinese Academy of Sciences, Beijing 100049, China

<sup>d</sup> College of Humanities and Sciences, Ajman University, Ajman 346, United Arab Emirates

<sup>e</sup> Nonlinear Dynamics Research Center (NDRC), Ajman University, Ajman 346, United Arab Emirates

### ARTICLE INFO

#### Keywords:

Transverse momentum spectra of particles  
Monte Carlo models prediction  
Collective phenomena  
Blast-wave model with Boltzmann–Gibbs statistics  
Kinetic freeze-out temperature  
Transverse flow velocity

### ABSTRACT

Analysis of the spectra of unidentified charged particles obtained by the CMS experiment in proton–proton collisions is reported in comparison with the simulation results of PYTHIA8.24 and EPOS-LHC models. The spectra obtained by the experiment were normalized to all non-single-diffractive (NSD) events using corrections for trigger and selection efficiency, acceptance, and branching ratios. The transverse-momentum ( $p_T$ ) spectra of the charged particles are measured in twelve equal bins of pseudorapidity ( $\eta$ ) from 0.0 to 2.4 for  $p_T$  from 0.1 to 2 GeV/c. The PYTHIA model reproduces the experimental data well in all bins of  $\eta$  especially in the region of high  $p_T$  while the EPOS model predicts well in the intermediate  $p_T$  regions. The intermediate regions where the EPOS model predicts well, broadens with increasing  $\eta$ .

We used the Blast-wave model with Boltzmann–Gibbs statistics to study collective properties of the hadronic matter and for better comparison of the models' prediction with the experimental data while determining the values of kinetic freeze-out temperature ( $T_0$ ) and transverse flow velocity ( $\beta_T$ ) for data and models. The values of  $T_0$  decrease with increasing  $\eta$  for data as well as for both the models. The transverse flow velocity has no clear trend with increasing  $\eta$  but a run through shows an increasing trend in the case of the data and the PYTHIA model but a decreasing trend in the case of the EPOS model. The multiplicity parameter  $N_0$  increases with increasing  $\eta$  and its values obtained by the fit function for the PYTHIA are closer to the ones obtained for data than the EPOS. It is concluded that none of the models completely describes the data in all bins of  $\eta$  over the entire  $p_T$  range but the PYTHIA has better prediction than the EPOS model because the former has implied flow-like effects and formation of color string resulting from multiple hard sub-collisions between final and initial partons (color reconnection) from independent hard scatterings due to which the model predicts the data well.

### Introduction

The study of particle production in  $pp$  collisions has two main motivations. In the first place, such studies are essential to distinguish hard hadronic interactions from the soft one which is used to tune phenomenological models for the description of final state observables. The particles can be well described by the Statistical models, while to compute the complete particle spectra, microscopic (string) models [1,2] are used. In the second place, it is used as a reference for the effect relevant to the collision of heavy ions at high energies to search for collective medium effects [3]. The  $pp$  studies themselves showed collective effects, which are normally expected in collisions

of heavy nuclei. Recent progress in high-energy  $pp$  collisions show that QGP droplets are expected to be formed in high-multiplicity  $pp$  collisions [4,5].

Quark–Gluon plasma can be produced by colliding heavy nuclei at high energies after attaining the condition of extreme temperature and high energy density. The QGP is a very short-lived state which is believed to be formed at the very early stages of the collisions. The system cools down and a hadron gas system is formed after expansion of the QGP matter [6,7]. During the evolution of the collision system, the information about the initial conditions of the system is lost due to multipartonic interactions. The final state information of the emitted

\* Corresponding authors.

E-mail addresses: [ajaz@awkum.edu.pk](mailto:ajaz@awkum.edu.pk) (M. Ajaz), [waqas\\_phy313@ucas.ac.cn](mailto:waqas_phy313@ucas.ac.cn) (M. Waqas).

particles is collected from the transverse momentum spectra. The information is very important for understanding the nature and behavior of the particles produced during high-energy collisions. After the collision, when the system evolves in space and time, then the system passes through chemical freeze-out and kinetic freeze-out stages. After the collision, the hot and dense system first attain the chemical equilibrium then expands due to cooling, thereby ceasing the inelastic collisions where the system size becomes equivalent to the mean free path. This is the chemical freeze-out state in which the abundance of all particles becomes constant. After this stage, the particles continue to collide with each other until their potency has no significance on the final state. The state where no more interactions between the particles occur and the transverse momentum distributions of the particles stay unchanged is named as kinetic freeze-out stage.

There are many statistical models used to explain the transverse momentum distributions of particles like Blast-wave model [8,9], Tsallis distributions [10,11],  $m_T$ -exponential distribution [12], Boltzmann–Gibbs, Einstein–Dirac distribution, and Erlang distribution [13]. Physical parameters can be extracted by fitting data with these statistical models.

In the present work, the spectra are in the low  $p_T$  range, therefore we would only need the soft excitation process for which the Blast-wave model with Boltzmann–Gibbs statistics is a better choice in our opinion because it works very well at low  $p_T$  range and is very close to an ideal gas model. Furthermore, it is easy to use it due to fewer free parameters. The current analysis at higher energy is a continuation of our work on the analyses of the  $p_T$  distribution of charged particles in different  $\eta$  bins at 0.9, and 2.36 TeV [14].

The rest of the paper is organized as follows. Section “Method and models” consists of the models and methods, followed by the results and discussion in Section “Results and discussion”, and the last section is summary and conclusions.

## Method and models

Transverse momentum spectra of unidentified charged particles in the pseudorapidity range of  $0 < \eta < 2.4$ , divided into twelve equal bins of width 0.2, simulated in two event generators; PYTHIA (PYTHIA8.24) [1] and EPOS (EPOS-LHC) [15] are contrasted with the data measured by the CMS experiment [16]. Both of the models are minimum bias for hadronic interactions with the following physics description.

PYTHIA is a general-purpose event generator for the production of particles at high energies. It is used by many of the experimental groups to validate the experimental data. It has the flexibility to study the hard and soft physics processes. PYTHIA was initially designed to study the color flow in hadronic collisions. It is based on the LUND string model [17] to study the string fragmentation, flow effects, beam remnants, and scattering. The initial and final state radiations along with the MPI model provide a good description of collision systems [18]. It includes the flavor and color correlations in its recent developments which is a very important study for the hadronic interactions. The data obtained at the LHC are argumentative intent with the possible existence of flow in  $pp$  collisions and can be studied by tuning the PYTHIA with color reconnection. It will make it possible to study flow-like effects coming from color string formation and multiple hard sub-collisions between the initial and final partons from independent hard scatterings inside the PYTHIA framework [19].

The EPOS model [16] is also a minimum bias event generator for hadronic interactions and can be used to study the cosmic ray air showers as well as heavy-ion collisions. EPOS is a unified approach that can predict minimum bias event particles with  $p_T$  from zero to a few GeV/c. EPOS models use a simplified treatment of QGP in events where the energy density is high enough (including in  $pp$ ). It is used to validate the data coming from the LHC in all collision systems after applying some modifications. Collective effects are more or less

important in all collision systems, so EPOS considers these effects by creating a medium. The model is based on the Gribov–Regge approach in which multiple pomerons exchange between  $pp$  collisions having Regge amplitudes [20,21]. If nuclear fusion is switched off in EPOS then it is comparable to the PYTHIA model (no final state interaction). For ease of writing, we used EPOS instead of the EPOS, the version used in the current manuscript, consistently throughout the manuscript.

The PYTHIA model which is QCD based has many advanced features to study the small system in detail like multiparton interactions, color re-connection. Flow-like features can also be studied using the PYTHIA model. While the EPOS model provides a good description of main hadronic particle production as it constrains from Modeling (mainly Glauber+Gribov) and extensive air shower data which are useful at the LHC. It works over a wide range in primary energies and for a variety of projectile/target combinations (without re-tuning), [21]. Again for simplicity, we used PYTHIA instead of the PHYTHIA8.24 version of the model throughout the manuscript. In the case of both event generators, we have simulated one million events for comparison with the experimental data [16].

Furthermore, to better compare the models’ prediction with the data, we used the Blast-wave model with Boltzmann–Gibbs statistics to fit the data and models prediction. Blast-wave model with Boltzmann–Gibbs statistics (BGBW) is a hydrodynamic model which has a strong assumption of local thermal equilibrium of a system at some instant of time and then experiences hydrodynamic evolution. The  $p_T$  distribution of BGBW model [22–24] is represented as

$$f_1(p_T) = \frac{1}{N} \frac{dN}{dp_T} = C p_T m_T \int_0^R r dr \times I_0 \left[ \frac{p_T \sinh(\rho)}{T_0} \right] K_1 \left[ \frac{m_T \cosh(\rho)}{T_0} \right], \quad (1)$$

where  $N$  display the number of particles,  $C$  being the constant of normalization and  $m_T = \sqrt{p_T^2 + m_0^2}$  is the transverse mass. In the present work, we used  $m_0$  equals the pion mass. The  $I_0$  and  $K_1$  are the modified Bessel functions of the first and second kinds respectively,  $\rho = \tanh^{-1}[\beta(r)]$  is the boost angle,  $\beta(r)$  is a self-similar flow profile which is given as  $\beta(r) = \beta_S(r/R)^{n_0}$ ,  $\beta_S$  is the flow velocity on the surface, while  $r/R$  is the relative radial position in the thermal source. There is the relation between  $\beta_T$  and  $\beta(r)$ ,  $\beta_T = (2/R^2) \int_0^R r \beta(r) dr = 2\beta_S/(n_0 + 2)$ . In the present work,  $n_0 = 2$  [22] is taken, which results in  $\beta_T = 0.5\beta_S$ . Indeed  $n_0$  can be a free parameter [23,25]. Mostly in literature,  $n_0 = 1$  or 2 is used. We choose  $n_0 = 2$  because it has closely resemblance with the hydrodynamic profile [22]. We can choose  $n_0 = 1$  also, which is the closest approximation to hydrodynamic at freeze-out [26]. The selection of  $n_0 = 1$  or 2 does not have a significant difference in the results which is reported in our recent work [27]. The freeze-out parameters are extracted from the transverse momentum spectra by the method of least square. Generally, the  $p_T$  spectra of the particles contribute to soft excitation and hard scattering processes. The former contributes to the narrow  $p_T$  spectrum, while the latter contributes to the spectrum in a wide range. BGBW model contributes to the soft excitation process, however, the Hagedorn function (which is an inverse power law) [28–30] can be used for the hard scattering process. The whole phenomenology of the BGBW model is presented in our previous works, and for more detail, interested readers are referred to Ref. [31].

## Results and discussion

Simulated results of the transverse momentum spectra of charged particles are contrasted with the measured spectra of CMS experiment in  $pp$  collisions [16] at 7 TeV. The spectra is presented in small bins of pseudorapidity divided into twelve equal regions of  $\eta$ ,  $0 \leq \eta \leq 2.4$  in  $p_T$  region of 0.1–2 GeV/c. Same cuts values including the exact region of pseudorapidity bins of  $\eta = 0.1, 0.3, 0.5, 0.7, 0.9, 1.1, 1.3, 1.5, 1.7, 1.9, 2.1, \text{ and } 2.3$  with  $p_T$  from (0.1–2) GeV/c are used in the

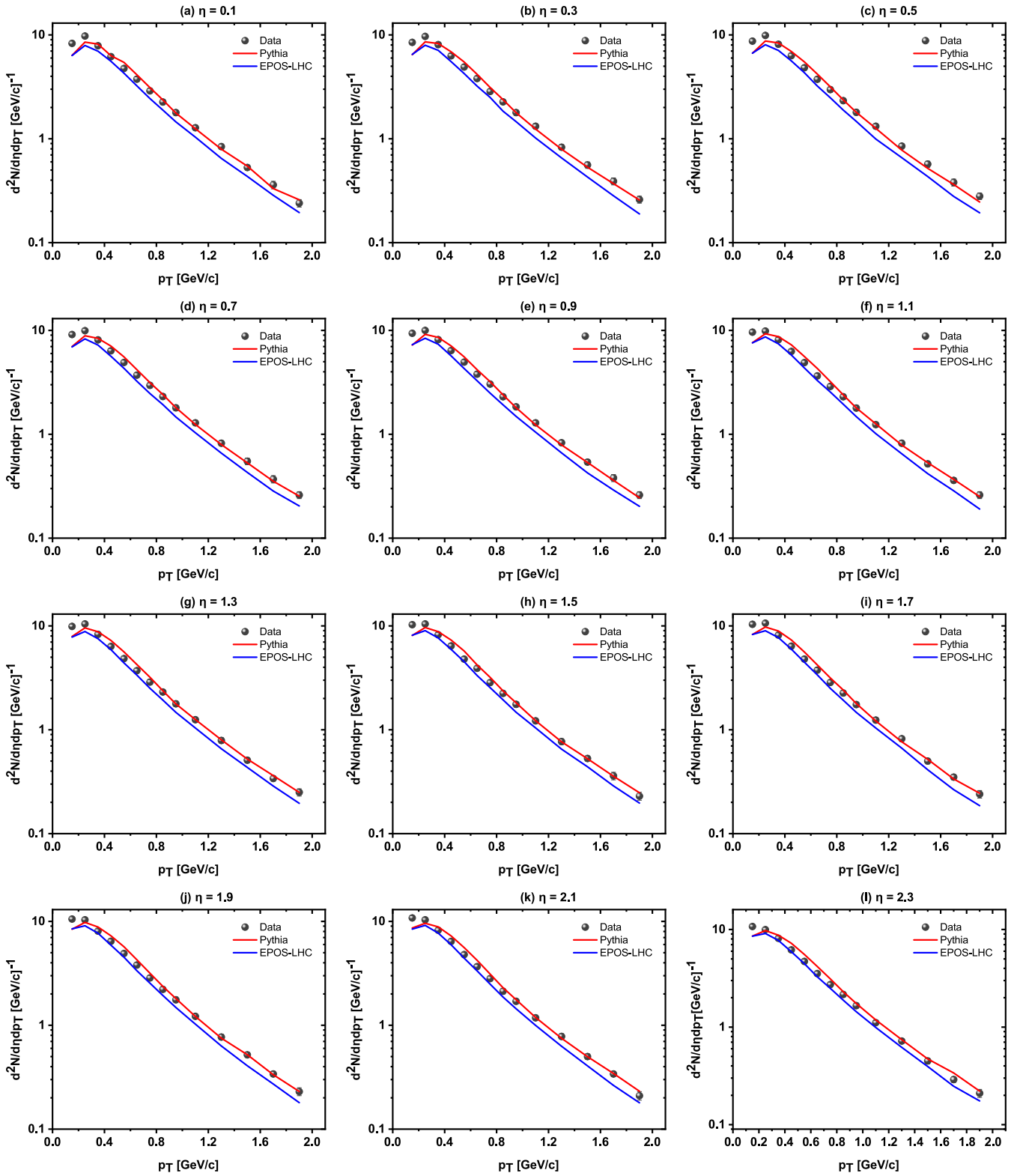


Fig. 1. The simulation prediction of PYTHIA and EPOS, transverse momentum distributions of charged particles, in twelve equal region of pseudorapidity from  $\eta = 0.1$  ( $0.0 \leq \eta \leq 0.2$ ) to  $\eta = 2.3$  ( $2.2 \leq \eta \leq 2.4$ ) are shown against the measurements of CMS experiment [16]. Filled dark gray color circles show the experimental data while red and blue lines are used to show the PYTHIA and EPOS models simulation.

simulations as in the experimental data. The  $p_T$  distributions of charged particles are shown in Fig. 1 in the region of aforementioned bins of  $\eta$ . Filled circles with dark gray colors are used to show the experimental data whereas lines of different colors show the prediction of models. Red and blue colors respectively are used to represent the PYTHIA

and EPOS model prediction. Systematic uncertainties are shown as vertical lines at each point in the experimental data as data errors. The systematic uncertainties of the quantities measured arise due to various corrections, selection of their event, and the MC model(s) used. A complete description of the systematic uncertainties, used in the current

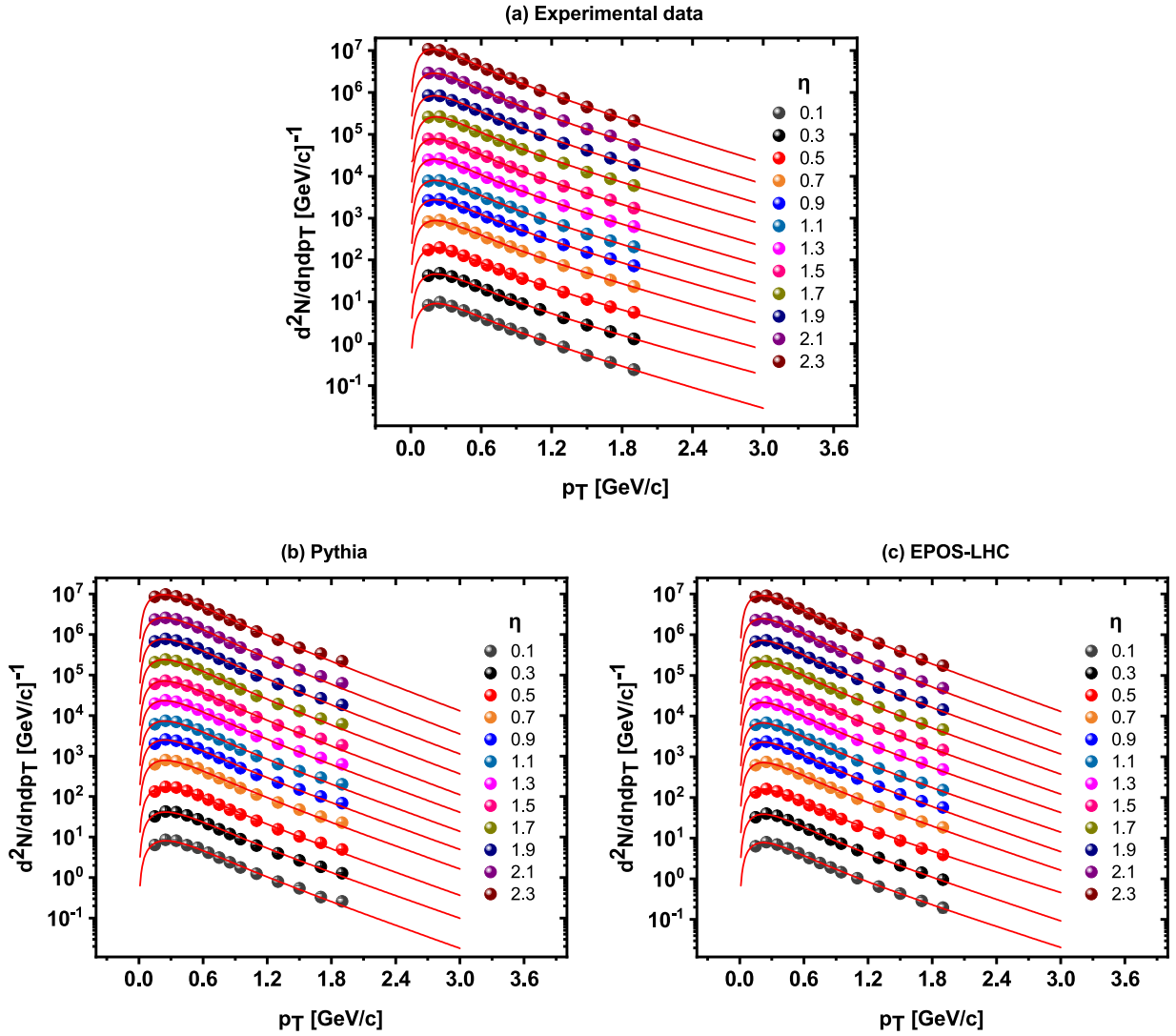


Fig. 2. Results of the fit function on the transverse momentum spectra of all charged particles on (a) Experimental data (b) PYTHIA model and (c) EPOS model. Markers of different colors are used to show the data for different  $\eta$  regions while curves are the results of the fit function.

study for analyses, averaged over  $\eta$  and  $p_T$  [16] are explained and tabulated as Table 3 in ref [32]. Since a million simulation events are used in the case of models, therefore the statistical errors in the models are very small and insignificant. For  $p_T > 0.7$  GeV/c, the PYTHIA model reproduces the data in all bins of the pseudorapidity. For the region of  $p_T$ ,  $0.3 \leq p_T \leq 0.7$  GeV/c, the model overestimates the measurements for about 8% while underestimates in the region for  $p_T < 0.3$  GeV/c for about 20%. The aforementioned observation is not affected by the different regions of  $\eta$  and hence the PYTHIA models have almost similar predictions in the rest of the  $\eta$  regions as well. The EPOS model, on the other hand, underestimates the measurements by about 20% for the low and high  $p_T$  ranges while reproducing good results in the intermediate region. It is further observed, that the intermediate region, where the prediction of the EPOS model is good, broadened with increasing the values of  $\eta$ .

Models based on statistical hadronization were successful in describing the low energy  $pp$  collision [33,34]. Naively, the formation of a system with quark-gluon plasma or hydrodynamics collective effects is not anticipated in  $pp$  collisions. Recently in Ref. [35], it has been reported that there is no radial flow effects at  $\sqrt{s_{NN}} = 200$  GeV and 540 GeV in  $pp$  collision. Nevertheless, the formation probability of such a system in  $pp$  collision on small scale cannot be ignored [36–39]. The  $pp$  collision with high multiplicity produced high energy density at SPS

(CERN) [40,41] encouraged scientists for deconfinement in hadronic collisions at SPS-CERN [36] and Fermilab-Tevatron [37,38]. Results obtained for flow velocity of hadrons found from the  $p_T$  spectra of these analyses are reported in [37] had been ascribed to as a signal of collective behavior, which is a characteristic of QGP formation [42]. In nuclear collisions (A-A), there is a large transverse flow velocity due to high energy density and the system easily thermalizes. On the other hand, in  $pp$  collisions, although there is a small flow, we use the grand canonical ensemble and the flow becomes large and the system is easy to thermalize.

Therefore an effort has been made to get a detailed comparison of the model's prediction with the data by using the fit of data and models prediction by the same function to get information about the collective behavior of the hadronic matter produced in  $pp$  collision at 7 TeV. We used the Blast-wave model with Boltzmann–Gibbs statistics to fit the data and models prediction, and the results are shown in Figs. 2. Fig. 2(a) is the fit result of the function on data while Fig. 2(b) and 2(c) are the fit results on the prediction of PYTHIA and EPOS models. The data and models predictions are shown by markers of different colors for different slices of  $\eta$  and the solid curve line is the result of the fit function.

The curves show that the function fits the data very well. The values of the parameter extracted from the data and models prediction by the

**Table 1**  
The values of free parameters ( $T_0$  and  $\beta_T$ ), normalization constant ( $N_0$ ) at different  $\eta$  intervals using Blastwave model with Boltzmann–Gibbs statistics.

Model	$\eta$	$N_0$	$\beta_T$ (c)	$T_0$ (MeV)	$\chi^2/ndf$
CMS Data	0.0–0.2	92.5 ± 0.1	0.455 ± 0.002	121.02 ± 0.01	3.3402/12
	0.2–0.4	93.9 ± 0.1	0.462 ± 0.002	118.09 ± 0.01	2.6008/12
	0.4–0.6	95.0 ± 0.1	0.463 ± 0.002	117.01 ± 0.01	3.0806/12
	0.6–0.8	96.0 ± 0.1	0.461 ± 0.002	115.05 ± 0.01	1.7417/12
	0.8–1.0	96.9 ± 0.2	0.463 ± 0.002	113.15 ± 0.01	1.5605/12
	1.0–1.2	96.4 ± 0.2	0.463 ± 0.001	111.09 ± 0.01	2.3937/12
	1.2–1.4	97.8 ± 0.1	0.464 ± 0.001	108.94 ± 0.01	3.2155/12
	1.4–1.6	98.6 ± 0.1	0.464 ± 0.001	107.22 ± 0.01	2.9279/12
	1.6–1.8	98.7 ± 0.1	0.464 ± 0.002	107.01 ± 0.03	3.9212/12
	1.8–2.0	98.5 ± 0.1	0.462 ± 0.001	107.92 ± 0.01	3.1628/12
PYTHIA Model	2.0–2.2	98.6 ± 0.2	0.463 ± 0.001	104.84 ± 0.01	3.5307/12
	2.2–2.4	97.0 ± 0.1	0.464 ± 0.001	100.88 ± 0.01	2.9055/12
	0.0–0.2	88.7 ± 0.1	0.407 ± 0.002	152.35 ± 0.02	8.9073/12
	0.2–0.4	90.5 ± 0.1	0.413 ± 0.002	150.11 ± 0.02	10.3518/12
	0.4–0.6	91.4 ± 0.1	0.412 ± 0.002	148.05 ± 0.02	8.3987/12
	0.6–0.8	92.7 ± 0.1	0.414 ± 0.002	146.01 ± 0.02	7.3881/12
	0.8–1.0	94.1 ± 0.1	0.415 ± 0.002	144.15 ± 0.02	7.0339/12
	1.0–1.2	96.0 ± 0.1	0.415 ± 0.002	143.01 ± 0.02	6.2002/12
	1.2–1.4	96.8 ± 0.1	0.415 ± 0.002	141.32 ± 0.02	5.4846/12
	1.4–1.6	97.6 ± 0.1	0.412 ± 0.001	140.72 ± 0.02	5.6939/12
EPOS Model	1.6–1.8	98.0 ± 0.1	0.413 ± 0.001	139.42 ± 0.01	4.9772/12
	1.8–2.0	98.3 ± 0.1	0.413 ± 0.001	138.52 ± 0.01	3.8838/12
	2.0–2.2	97.5 ± 0.1	0.412 ± 0.001	137.44 ± 0.01	4.4104/12
	2.2–2.4	97.2 ± 0.1	0.415 ± 0.001	135.55 ± 0.02	3.4710/12
	0.0–0.2	78.3 ± 0.1	0.448 ± 0.001	123.8 ± 0.02	5.2179/12
	0.2–0.4	77.9 ± 0.1	0.445 ± 0.001	124.17 ± 0.01	4.3262/12
	0.4–0.6	79.2 ± 0.2	0.453 ± 0.001	121.11 ± 0.02	4.8375/12
	0.6–0.8	80.2 ± 0.2	0.449 ± 0.002	121.05 ± 0.02	3.2554/12
	0.8–1.0	81.4 ± 0.1	0.449 ± 0.001	120.85 ± 0.02	2.2421/12
	1.0–1.2	82.9 ± 0.1	0.447 ± 0.001	119.21 ± 0.02	1.7147/12
PYTHIA Model	1.2–1.4	84.2 ± 0.1	0.446 ± 0.001	119.15 ± 0.02	1.8844/12
	1.4–1.6	86.1 ± 0.1	0.446 ± 0.001	117.16 ± 0.01	1.7442/12
	1.6–1.8	85.8 ± 0.1	0.445 ± 0.001	116.48 ± 0.02	1.1101/12
	1.8–2.0	86.2 ± 0.1	0.445 ± 0.001	115.85 ± 0.01	0.7537/12
	2.0–2.2	86.2 ± 0.1	0.443 ± 0.001	115.35 ± 0.001	1.5548/12
	2.2–2.4	86.3 ± 0.1	0.443 ± 0.001	115.11 ± 0.01	1.1373/12

function are given in the Table 1. The last column in the Table 1 shows the values of  $\chi^2/ndf$  which confirms that the function fits the data very well. The second last column shows the values of kinetic freeze-out temperature ( $T_0$ ). The value of  $T_0$  decreases with increasing  $\eta$  from (121.02 ± 0.002) MeV to (100.88 ± 0.01) for experimental data, from (152.35 ± 0.02) MeV to (135.55 ± 0.02) MeV for PYTHIA model and from (124.17 ± 0.01) MeV to (115.11 ± 0.01) MeV for EPOS model. Furthermore, it is observed that the values of the EPOS model are closer to the values extracted by the function for the data than the PYTHIA model. The values of  $T_0$  decrease monotonically in all the cases with increasing  $\eta$ . It is because an increase in  $\eta$  yields a decrease in the system transfer energy as a consequence of larger penetration among participating nucleons. It should be noted that here the large penetration refers to large rapidity shift. The transverse flow velocity has no clear trend with increasing  $\eta$  which is also reported in [43] at low energy as well. In literature, one can also find a decreasing trend of  $\beta_T$  with decreasing centrality [31]. A closer look shows an increasing trend in the case of data and the PYTHIA model but a decreasing trend in the EPOS model.  $\beta_T$  increases from (0.455 ± 0.002) c to (0.464 ± 0.001) c in case of data and from (0.407 ± 0.002) c to (0.415 ± 0.001) c in PYTHIA but decreases in EPOS from (0.448 ± 0.001) c to (0.443 ± 0.001) c. It is worth mentioning that the values of  $\beta_T$  extracted from the EPOS model are closer to that of the experimental data than the PYTHIA model but the latter has the same increasing trend while the former has opposite trend of  $\beta_T$ . Comparing the values of  $\beta_T$  and  $T_0$  obtained here with our previous work [44] show that the values of the two parameters increase with increasing the center of mass energy which is due to the reason that the system gets higher degree of excitation as the collision energy increases.  $N_0$ , the normalization constant, is a multiplicity parameter [45,46] and it has an increasing effect with  $\eta$ . The values of  $N_0$  obtained by the

fit function for PYTHIA are closer to the ones obtained for data than the EPOS. As mentioned above that the PYTHIA model reproduced the data well in comparison to the EPOS model which is supported by the parameter  $N_0$  extracted from the fit function.

## Summary and conclusion

In this work, we reported the simulation results of the  $p_T$  spectra of the unidentified charged particles in comparison with the measured experimental data at 7 TeV. One million simulation events were used in the case of the PYTHIA and EPOS model for comparison with the experimental data. The spectra obtained by the experiment were normalized to all non-single-diffractive (NSD) events using corrections for trigger and selection efficiency, acceptance, and branching ratios. We used the same cuts and conditions that were used in measuring the experimental data that include the number and size of  $\eta$  bins and the  $p_T$  range. Small bins of pseudorapidity ( $\eta$ ) divided into twelve equal slices were used from 0.0 <  $\eta$  < 2.4 of width 0.2 each for  $p_T = 0.1$  to 2 GeV/c. The PYTHIA model reproduced the experimental data well in all  $\eta$  bins especially in the region of high  $p_T$ , for  $p_T > 0.7$  GeV/c while the EPOS underestimates. The EPOS model reproduce good results in the intermediate  $p_T$  region. It has further been found that the region of good prediction by the EPOS model broadened towards higher  $p_T$  with increasing  $\eta$ .

Furthermore, we used the Blastwave model with Boltzmann–Gibbs statistics to study collective properties of the hadronic matter and for better comparison of the models' prediction with the experimental data while determining the values of  $T_0$  and  $\beta_T$  for data and models. The kinetic freeze-out temperature ( $T_0$ ) decreases with increasing  $\eta$  while the transverse flow velocity has no clear trend with increasing  $\eta$  but

a run through shows an increasing trend in case of data and PYTHIA model but a decreasing trend in EPOS model.  $N_0$ , the normalization constant, shows the multiplicity and has an increasing effect with  $\eta$ . The value of  $N_0$  obtained by the fit function for PYTHIA is closer to the ones obtained for data than the EPOS. It is concluded that none of the models completely describe the data over the entire  $p_T$  range in the small slices of  $\eta$  but PYTHIA has a better prediction of the data than the EPOS. The PYTHIA model has implied flow-like effects resulting from multiple hard sub-collisions and formation of color string between final and initial partons (color reconnection) from independent hard scatterings due to which the model predicts the data well.

### CRedit authorship contribution statement

**Muhammad Ajaz:** Wrote the main manuscript text, simulations and analysis, Prepared figures and interpreted the results, Reviewed the manuscript. **Ahmed M. Khubrani:** Wrote the main manuscript text, simulations and analysis, Reviewed the manuscript. **Muhammad Waqas:** Wrote the main manuscript text, Prepared figures and interpreted the results, Reviewed the manuscript. **Abd Al Karim Haj Ismail:** simulations and analysis, Reviewed the manuscript. **Elmuez A. Dawi:** Reviewed the manuscript.

### Declaration of competing interest

The authors declare that they have no known competing financial interests or personal relationships that could have appeared to influence the work reported in this paper.

### Availability of data and materials

All data generated or analyzed during this study are included in this published article

### Acknowledgment

The authors would like to acknowledge Abdul Wali Khan University Mardan for providing all possible facilities and the support of Ajman University Internal Research Grant No. DGSR Ref. 2021-IRG-HBS-12.

### Funding

Ajman University Internal Research Grant No. DGSR Ref. 2021-IRG-HBS-12.

### References

- [1] Sjöstrand T, Ask S, Christiansen JR, Corke R, Desai N, Ilten P, et al. An introduction to PYTHIA 8.2. *Comput Phys Comm* 2015;191:159–77. <http://dx.doi.org/10.1016/j.cpc.2015.01.024>.
- [2] Vovchenko V, Begun VV, Gorenstein MI. Hadron multiplicities and chemical freeze-out conditions in proton-proton and nucleus-nucleus collisions. *Phys Rev C* 2016;93:064906. <http://dx.doi.org/10.1103/PhysRevC.93.064906>.
- [3] Drescher H, Hladik M, Ostapchenko S, Pierog T, Werner K. Parton-based Gribov-Regge theory. *Phys Rep* 2001;350(2):93–289. [http://dx.doi.org/10.1016/S0370-1573\(00\)00122-8](http://dx.doi.org/10.1016/S0370-1573(00)00122-8).
- [4] Sahu D, Sahoo R. Characterizing proton-proton collisions at the large hadron collider with thermal properties. *Physics* 2021;3(2):207–19. <http://dx.doi.org/10.3390/physics3020016>.
- [5] Olimov KK, Liu F-H, Musaev KA, Olimov K, Tukhtaev BJ, Yuldashev BS, et al. Multiplicity dependencies of midrapidity transverse momentum spectra of identified charged particles in p+p collisions at  $(s)_{1/2}=13$  TeV at LHC. *Internat J Modern Phys A* 2021;36(20):2150149. <http://dx.doi.org/10.1142/S0217751X21501499>.
- [6] Busza W, Rajagopal K, van der Schee W. Heavy ion collisions: The big picture and the big questions. *Ann Rev Nucl Part Sci* 2018;68(1):339–76. <http://dx.doi.org/10.1146/annurev-nucl-101917-020852>.
- [7] Niida T, Miale Y. Signatures of QGP at RHIC and the LHC. *AAPPS Bull* 2021;31:2309–4710. <http://dx.doi.org/10.1007/s43673-021-00014-3>.
- [8] Waqas M, Peng G-X. Study of dependence of kinetic freezeout temperature on the production cross-section of particles in various centrality intervals in Au–Au and Pb–Pb collisions at high energies. *Entropy* 2021;23(4).
- [9] Waqas M, Peng GX, Wang R-Q, Ajaz M, Haj Ismail AAK. Freezeout properties of different light nuclei at the RHIC beam energy scan. *Eur Phys J Plus* 2021;136:1082. <http://dx.doi.org/10.1140/epjp/s13360-021-02089-1>.
- [10] Mathai A, Haubold H. Pathway model, superstatistics, tsallis statistics, and a generalized measure of entropy. *Physica A* 2007;375(1):110–22. <http://dx.doi.org/10.1016/j.physa.2006.09.002>.
- [11] Li L-L, Liu F-H, Waqas M, Ajaz M. Analyzing transverse momentum spectra by a new method in high-energy collisions. *Universe* 2022;8(1). <http://dx.doi.org/10.3390/universe8010031>.
- [12] Li C-S, Rather NA, Rather TA. New generalizations of exponential distribution with applications. *J Probab Stat* 2017;2106748. <http://dx.doi.org/10.1155/2017/2106748>.
- [13] Adamczyk L, et al., STAR Collaboration Collaboration. Bulk properties of the medium produced in relativistic heavy-ion collisions from the beam energy scan program. *Phys Rev C* 2017;96:044904. <http://dx.doi.org/10.1103/PhysRevC.96.044904>.
- [14] Yang P-P, Ajaz M, Waqas M, Liu F-H, Suleymanov M. Pseudorapidity dependence of the  $p_T$  spectra of charged hadrons in pp collisions at  $\sqrt{s}=0.9$  and 2.36 TeV. *J Phys G: Nucl Part Phys* 2022. <http://dx.doi.org/10.1088/1361-6471/ac5d0b>.
- [15] Pierog T, Karpenko I, Katzy JM, Yatsenko E, Werner K. EPOS LHC: Test of collective hadronization with data measured at the CERN large hadron collider. *Phys Rev C* 2015;92(3):034906. <http://dx.doi.org/10.1103/PhysRevC.92.034906>.
- [16] Khachatryan V, et al., CMS Collaboration. Transverse-momentum and pseudorapidity distributions of charged hadrons in pp collisions at  $\sqrt{s} = 7$  TeV. *Phys Rev Lett* 2010;105:022002. <http://dx.doi.org/10.1103/PhysRevLett.105.022002>.
- [17] Andersson B, Gustafson G, Ingelman G, Sjöstrand T. Parton fragmentation and string dynamics. *Phys Rep* 1983;97(2):31–145. [http://dx.doi.org/10.1016/0370-1573\(83\)90080-7](http://dx.doi.org/10.1016/0370-1573(83)90080-7).
- [18] Sjostrand T, Mrenna S, Skands PZ. PYTHIA 6.4 Physics and manual. *J High Energy Phys* 2006;05:026. <http://dx.doi.org/10.1088/1126-6708/2006/05/026>.
- [19] Maldonado-Cervantes IA, Cuautele E, Paic G, Velasquez AO, Christiansen P. Color reconnection and flow-like patterns in pp collisions. *J Phys Conf Ser* 2014;509:012064. <http://dx.doi.org/10.1088/1742-6596/509/1/012064>.
- [20] Pierog T, Karpenko I, Katzy JM, Yatsenko E, Werner K. EPOS LHC: Test of collective hadronization with data measured at the CERN large hadron collider. *Phys Rev C* 2015;92:034906. <http://dx.doi.org/10.1103/PhysRevC.92.034906>.
- [21] Drescher H, Hladik M, Ostapchenko S, Pierog T, Werner K. Parton-based Gribov-Regge theory. *Phys Rep* 2001;350(2):93–289. [http://dx.doi.org/10.1016/S0370-1573\(00\)00122-8](http://dx.doi.org/10.1016/S0370-1573(00)00122-8).
- [22] Schnedermann E, Sollfrank J, Heinz U. Thermal phenomenology of hadrons from 200A GeV S+S collisions. *Phys Rev C* 1993;48:2462–75. <http://dx.doi.org/10.1103/PhysRevC.48.2462>.
- [23] Abelev BI, et al., STAR Collaboration Collaboration. Systematic measurements of identified particle spectra in pp, d + Au, and Au + Au collisions at the STAR detector. *Phys Rev C* 2009;79:034909. <http://dx.doi.org/10.1103/PhysRevC.79.034909>.
- [24] Abelev BI, et al., STAR Collaboration Collaboration. Identified particle production, azimuthal anisotropy, and interferometry measurements in Au+Au collisions at  $\sqrt{s_{NN}} = 9.2$  GeV. *Phys Rev C* 2010;81:024911. <http://dx.doi.org/10.1103/PhysRevC.81.024911>.
- [25] Petrovici M, Andrei C, Berceanu I, Bercuci A, Herghelegiu A, Pop A. Recent results and open questions on collective type phenomena from A-A to pp collisions. *AIP Conf Proc* 2015;1645(1):52–60. <http://dx.doi.org/10.1063/1.4909559>.
- [26] Kolb PF, Heinz U. Hydrodynamic description of ultrarelativistic heavy-ion collisions. 2003.
- [27] Waqas M, Haj Ismail AAK, Ajaz M, AbdelKader A. Excitation function of kinetic freeze-out parameters at 6.3, 17.3, 31, 900 and 7000 GeV. *Universe* 2022;8(2). <http://dx.doi.org/10.3390/universe8020138>.
- [28] Arnison G, et al. Transverse momentum spectra for charged particles at the CERN proton-antiproton collider. *Phys Lett B* 1982;118(1):167–72. [http://dx.doi.org/10.1016/0370-2693\(82\)90623-2](http://dx.doi.org/10.1016/0370-2693(82)90623-2).
- [29] Odorico R. Does a transverse energy trigger actually trigger on large-PT jets? *Phys Lett B* 1982;118(1):151–4. [http://dx.doi.org/10.1016/0370-2693\(82\)90620-7](http://dx.doi.org/10.1016/0370-2693(82)90620-7).
- [30] Hagedorn R. Multiplicities,  $p_T$  distributions and the expected hadron → quark - gluon phase transition. *Riv Nuovo Cimento* 1983;6N10:1–50. <http://dx.doi.org/10.1007/BF02740917>.
- [31] Muhammad W, Li B-C. Kinetic freeze-out temperature and transverse flow velocity in Au-Au collisions at RHIC-BES energies. *Adv High Energy Phys* 2020;2020:1–14. <http://dx.doi.org/10.1155/2020/1787183>.
- [32] Khachatryan V, et al., CMS Collaboration. Transverse-momentum and pseudorapidity distributions of charged hadrons in pp collisions at  $\sqrt{s} = 0.9$  and 2.36 TeV. *J High Energy Phys* 2010;41:1029–8479. [http://dx.doi.org/10.1007/JHEP02\(2010\)041](http://dx.doi.org/10.1007/JHEP02(2010)041).
- [33] Becattini F, Castorina P, Milov A, Satz H. A comparative analysis of statistical hadron production. *Eur Phys J C* 2010;66(3–4):377–86. <http://dx.doi.org/10.1140/epjc/s10052-010-1265-y>.

- [34] Kraus I, Cleymans J, Oeschler H, Redlich K. Particle production in  $p$ - $p$  collisions and predictions for  $\sqrt{s} = 14$  TeV at the CERN large hadron collider (LHC). *Phys Rev C* 2009;79:014901. <http://dx.doi.org/10.1103/PhysRevC.79.014901>.
- [35] Jiang K, Zhu Y, Liu W, Chen H, Li C, Ruan L, et al. Onset of radial flow in  $p+p$  collisions. 2014.
- [36] Van Hove L. Multiplicity dependence of  $pt$  spectrum as a possible signal for a phase transition in hadronic collisions. *Phys Lett B* 1982;118(1):138–40. [http://dx.doi.org/10.1016/0370-2693\(82\)90617-7](http://dx.doi.org/10.1016/0370-2693(82)90617-7).
- [37] Lévai P, Müller B. Transverse baryon flow as possible evidence for a quark-gluon-plasma phase. *Phys Rev Lett* 1991;67:1519–22. <http://dx.doi.org/10.1103/PhysRevLett.67.1519>.
- [38] Alexopoulos T, Anderson E, Bujak A, Carmony D, Erwin A, Gutay L, et al. Evidence for hadronic deconfinement in  $pp$  collisions at 1.8 TeV. *Phys Lett B* 2002;528(1):43–8. [http://dx.doi.org/10.1016/S0370-2693\(02\)01213-3](http://dx.doi.org/10.1016/S0370-2693(02)01213-3).
- [39] Weiner RM. Surprises from the search for quark-gluon plasma? when was quark-gluon plasma seen? *Internat J Modern Phys E* 2006;15(01):37–70. <http://dx.doi.org/10.1142/S0218301306004004>.
- [40] Alpgård K, et al. First results on complete events from  $pp$  collisions at the cm energy of 540 GeV. *Phys Lett B* 1981;107(4):310–4. [http://dx.doi.org/10.1016/0370-2693\(81\)90837-6](http://dx.doi.org/10.1016/0370-2693(81)90837-6).
- [41] Arnison G, et al. Some observations on the first events seen at the CERN proton-antiproton collider. *Phys Lett B* 1981;107(4):320–4. [http://dx.doi.org/10.1016/0370-2693\(81\)90839-X](http://dx.doi.org/10.1016/0370-2693(81)90839-X).
- [42] Ghosh P, Muhuri S, Nayak JK, Varma R. Indication of transverse radial flow in high-multiplicity proton-proton collisions at the large hadron collider. *J Phys G: Nucl Part Phys* 2014;41(3):035106. <http://dx.doi.org/10.1088/0954-3899/41/3/035106>.
- [43] Waqas M, Chen H-M, Peng G-X, Haj Ismail AAK, Ajaz M, Wazir Z, et al. Study of kinetic freeze-out parameters as a function of rapidity in  $pp$  collisions at CERN SPS energies. *Entropy* 2021;23(10):1363. <http://dx.doi.org/10.3390/e23101363>.
- [44] Ajaz M, Waqas M, Peng G, et al. Study of  $pT$  spectra of light particles using modified hagedorn function and cosmic rays Monte Carlo event generators in proton-proton collisions at  $\sqrt{s}=900$  GeV. *Eur Phys J Plus* 2022;137:52. <http://dx.doi.org/10.1140/epjp/s13360-021-02271-5>.
- [45] Waqas M, Peng GX, Liu F-H, Wazir Z. Effects of coalescence and isospin symmetry on the freezeout of light nuclei and their anti-particles. 2021, p. 2045–322, URL <https://doi.org/10.1038/s41598-021-99455-x>.
- [46] Waqas M, Peng GX, Liu F-H. An evidence of triple kinetic freezeout scenario observed in all centrality intervals in Cu–Cu, Au–Au and Pb–Pb collisions at high energies. *J Phys G: Nucl Part Phys* 2021;48(7):075108. <http://dx.doi.org/10.1088/1361-6471/abdd8d>.